Switchable two-dimensional gratings based on field-induced layer undulations in cholesteric liquid crystals

B. I. Senyuk, I. I. Smalyukh, and O. D. Lavrentovich

Liquid Crystal Institute and Chemical Physics Interdisciplinary Program, Kent State University, Kent, Ohio 44242

We propose switchable two-dimensional (2D) diffractive gratings with periodic refractive-index modulation arising from layer undulations in cholesteric liquid crystals. The cholesteric cell can be switched between two states: (1) flat layers of a planar cholesteric texture and (2) a square lattice of periodic director modulation associated with layer undulations that produces 2D diffraction patterns. The intensities of the diffraction maxima can be tuned by changing the applied field. The diffractive properties can be optimized for different wavelengths by appropriately choosing cholesteric pitch, cell thickness, and surface treatment. © 2005 Optical Society of America

OCIS codes: 050.1950, 160.3710.

Electrically controlled gratings are widely used for beam steering, optical waveguides, and splitting monochromatic beams. With the advent of multibeam devices, they became popular for beam multiplexing. Splitting the beam into a given number of beams by use of a two-dimensional (2D) grating is an efficient way to distribute an optical signal into an array of receivers. Liquid-crystal (LC) devices have great potential as electrically switchable 2D diffraction gratings. A 2D grating can be produced by orthogonally overlaying two one-dimensional (1D) structures.[1] This results in a rectangular diffraction pattern, and the grating efficiency is then a product of the efficiencies of two 1D gratings.[1] Another approach employs ordered LC droplet structures[2,3] in which the diffraction pattern is switched by changing the director field in the droplets. 2D diffraction can also be produced by use of a spatial light modulator.[4] On the other hand, 1D electrically controlled gratings based on periodically modulated textures in thin cholesteric cells[5,6] as well as polymer-stabilized,[7] polymer-dispersed,[8] and photocurable[9] LC gratings offer technological simplicity and good diffraction quality. We propose electrically controlled 2D gratings that employ layer undulations in cholesteric LCs.

The LC cells were constructed from glass substrates coated with transparent indium tin oxide patterned electrodes. The unidirectionally buffed thin layers of polyimide PI2555 (HD MicroSystem) were used to set the easy axis for LC molecules at the confining plates. The cell thicknesses varied in the range of $d = 5$–60 μm. In the LC mixtures (Table 1), cholesteric pitch p was varied from values much larger than the wavelength of the incident beam ($p \gg \lambda$) to much smaller values ($p < \lambda$). The nematic hosts E7, 5CB, and ZLI-3412 were doped with chiral agent CB15, and the nematic host BL015 was doped with ZLI-811 (all from EM Industries). The cholesteric mixtures were additionally doped with ~0.01% of the fluorescent dye BTBP (N, N'-bis(2,5-di-tert-butylphenyl)-3, 4, 9, 10-perylene-dicarboximide) for fluorescence confocal polarizing microscopy (FCPM) observations.[10]

At large scales ($p \ll d$) cholesterics can be described as lamellar phases[11] with the thickness of the layer equal to $p/2$. Similarly to other lamellar media, the layer undulations can be produced by various external factors including an electric field.[12–14] When no field is applied, the helical axis is perpendicular to the bounding plates and the average refractive index is uniform in the plane of a cell. In the applied electric field the LC molecules tend to reorient along the field. When the voltage reaches some critical value, the layer undulations occur[13,14] (Fig. 1). The threshold voltage for the appearance of undulations in the softly anchored cholesteric cells[15] is $U_u \propto d/[p(d + 2\xi)]^{1/2}$, where ξ is the anchoring extrapolation length characterizing cholesteric anchoring at the confining surfaces, usually $\sim p$.[12,16] In the studied cells with $d/p > 2.5$ the 2D patterns of undulations appear at $U_u = 3$–15 V. The two mutually orthogonal wave vectors of the patterns are at 45° to the rubbing directions in the cells with substrates rubbed in a perpendicular fashion. In the cells with antiparallel rubbing, one of the wave vectors is parallel to the rubbing and another is perpendicular to it. The difference between the spatial periods of undulations in two orthogonal directions is <1% (Fig. 1). The period of the square lattice is $L_u = C(6K_{33}/K_{22})^{1/4}[p(d + 2\xi)]^{1/2}$, where C is a constant of the order of unity that depends on surface anchoring and K_{22} and K_{33} are the twist and bend elastic constants, respectively.[15] L_u can be varied in the submicrometer–micrometer range by adjusting d, p, and the surface treatment. The patterns of undulations correspond to 2D spatial modulation of the director, the phase retardation, and the effective refractive index. The 2D undulations were stable for days without being spoiled by oily streaks.[17] The appearance of this type of defect is a nucleation process.[17] We avoided the oily streaks by eliminating the nucleation sites, such as surface irregularities, mechanical impurities, and strong layer distortions at the cell edges. Patterned electrodes helped prevent nucleation at the cell edge.

We studied the diffraction parameters with a setup consisting of an Ar laser ($\lambda = 488$ nm), a polarizer, a

Table 1.   Materials and Their Electro-Optic Characteristics

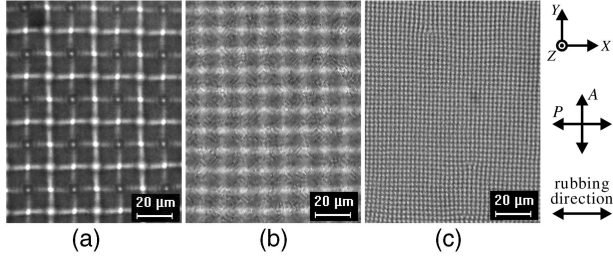| Nematic Host	Birefringence of Nematic Host, Δn	Dielectric Anisotropy of Nematic Host, $\Delta\epsilon$	Chiral Dopant, % by Weight	Pitch, μm
E7	0.224	13.8	CB15, ~2.7%	5
5CB	0.211	11.5	CB15, ~2.8%	5
ZLI-3412	0.078	3.4	CB15, ~3.2%	5
BL015	0.28	16	ZLI-811, ~30%	0.31

Fig. 1. Polarizing-microscopy textures of the 2D undulations in cholesteric cells under applied ac voltage $U(1\ \text{kHz})$: (a) E7 + CB15, $p = 5\ \mu$m, $d/p \approx 11$, $U = 12$ V; (b) 5CB + CB15, $p = 5\ \mu$m, $d/p \approx 2.5$, $U = 3.6$ V; (c) BL015 + ZLI-811, $p = 0.31\ \mu$m, $d/p \approx 40$, $U = 14$ V.

$\lambda/4$ plate, the cholesteric cell, and a screen. A photodetector was used to measure the intensity for each maximum of the diffraction pattern (Fig. 2). The combination of a polarizer and a $\lambda/4$ plate allowed us to tune the polarization state of the incident light from linear to circular. Diffraction angle θ for the first diffraction maximum was in the range of $\theta = 1°-15°$ for the Ar laser beam and up to 42° for an infrared beam at $\lambda \approx 3\ \mu$m (diode laser, Laser Components Instrument Group), depending on d and p. The observed diffraction pattern is well described by the diffraction conditions for maximum intensity

$$m\lambda = L_g \sin\theta, \tag{1}$$

where m is the diffraction order and, L_g is the grating periodicity. The positions of the intensity maxima satisfy the equations

$$r = \lambda D(m_x{}^2 + m_y{}^2)^{1/2}/L_g, \qquad \tan\varphi = m_y/m_x, \tag{2}$$

where r is the distance from the center to the intensity maximum, m_x and m_y are the diffraction orders in the X and Y directions, φ is the angle between the X axis and the vector connecting the zeroth and mth diffraction maxima, and D is the distance to the screen.

The diffraction pattern strongly depends on d/p. For cells with $2.5 < d/p < 10$ the intensities of the odd and even diffraction maxima are nonmonotonic functions of m_x and m_y [Fig. 2(a)], as in 1D cholesteric gratings.[6] The cells with $d/p > 10$ produce diffraction patterns in which the intensities of the maxima monotonically decrease with the increase of the diffraction order [Fig. 2(b)]. Clearly, the odd–even effect is a feature of the 2D gratings with a comparably small

number of layers ($d/p < 10$) and is not present for relatively thick samples of $d/p > 10$.

To gain insight into the odd–even effect, we use FCPM[10] for imaging of the director in the vertical cross sections of cells (Fig. 3). The cholesteric layer that is adjacent to the substrate is not flat, indicating that cholesteric anchoring is finite.[12,16] One can distinguish two different types of spatial distortion of the LC director and the average refractive index: one in the bulk region and another at the two surface regions. The modulation of the refractive index scales as $(\partial u/\partial x)^2$, where u is the displacement of layers from their unperturbed flat positions and $\partial u/\partial x$ is the layers' tilt with respect to the substrate. Therefore the grating in Fig. 3(a) can be considered qualitatively as comprised of three adjacent parts: two gratings created by the close-to-surface layers with a period of the refractive index of $L_g = L_u$ and the LC bulk grating with a period of the refractive index
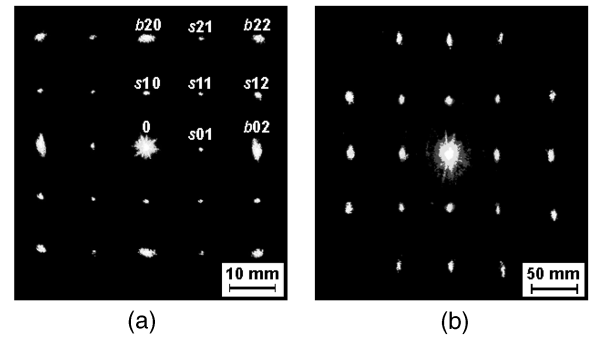

Fig. 2. Diffraction patterns obtained for cholesteric cells with (a) 5CB + CB15, $p = 5\ \mu$m, $d/p \approx 2.5$, $U = 3.6$ V; (b) BL015 + ZLI-811, $p = 0.31\ \mu$m, $d/p \approx 40$, $U = 14$ V. Distance to the screen is $D = 0.25$ m.

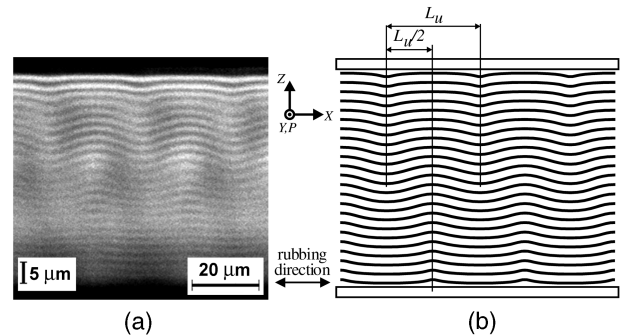
Fig. 3. (a) FCPM cross section of 2D undulations in the cholesteric cell with a mixture of ZLI-3412 + CB15 ($p = 5\ \mu$m, $d/p \approx 11$, $U = 12$ V) and (b) the reconstructed layer pattern. P marks the polarization direction of probing light in FCPM.

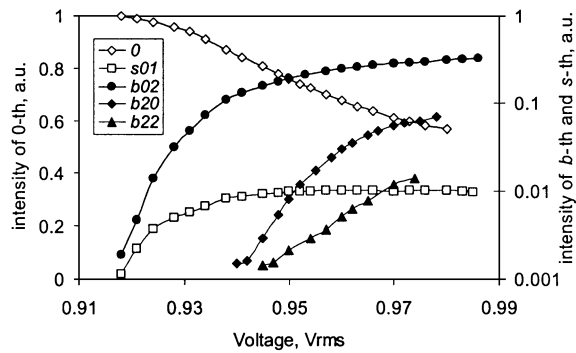Fig. 4. Intensities for different-order diffraction maxima versus voltage for the cholesteric cell with $d = 12.5$ μm and $p = 5$ μm.

of $L_g = L_u/2$. The two surface gratings are shifted by $L_u/2$ with respect to each other and separated by a distance of $\sim d$ along the Z axis. The resulting diffraction pattern is a superposition of diffraction effects caused by the three stacked gratings and can be described with Eqs. (1) and (2). The diffracted beams labeled b [Fig. 2(a)] are caused by modulation of the refractive index in the bulk with a period of $L_u/2$ and the beams labeled s [Fig. 2(a)] are caused by modulation of the refractive index close to surfaces with period L_u. When d/p is large, the contribution from the regions close to the surfaces is negligible compared with the modulation of the refractive index in the bulk of the cell, and the diffraction maxima caused by the close-to-surface layers are not observed [Fig. 2(b)]. Thus the alternation of strong- and weak-intensity maxima in the diffraction pattern is caused by the surface confinement, similar to the case of 1D gratings.[6]

When the applied voltage is changed, the layer undulations become more or less pronounced and, as a consequence, the depth of the modulation of the effective refractive index changes too. Therefore the intensities of the high-order maxima can be controlled with the voltage (Fig. 4). Importantly, the performance of the gratings was found to be practically polarization independent and the relative intensities of the diffraction maxima did not change much after the linear polarization state was switched between the two orthogonal directions (up to 5%) or the polarization was changed from linear to circular (up to 10%). The diffraction pattern is stable in a wide voltage range. For example, 55-μm-thick cells with an E7 + CB15 mixture of $p = 5$ μm produce the diffraction pattern within a voltage range of $U = 12-25$ V in which one can control the intensities of the high-order maxima.

Depending on parameter $\kappa = \lambda d/L_g^2$, one can distinguish the Raman–Nath ($\kappa \ll 1$) and Bragg ($\kappa > 1$) types of diffraction.[18] In the case of thick cholesteric cells with $d \gg \xi$ and $L_g = L_u/2$, assuming elastic constants for a 5CB matrix ($K_{22} = 3$ pN, $K_{33} = 10$ pN), one obtains $L_g \approx 1.1(pd)^{1/2}$ and $\kappa_{\text{thick}} \approx 0.9\lambda/p$. In the thin cells with $d \sim \xi$ and $L_g = L_u$ we find $\kappa_{\text{thin}} \approx 0.2\lambda d/[\,p(d + 2\xi)]$. The layer undulations can be used as gratings of both types.[18] The conditions for the Bragg diffraction are achievable, especially with

small p and λ in the infrared region. For example, for $p = 0.31$ μm and $\lambda = 3$ μm one obtains $\kappa_{\text{thick}} \approx 9$, which corresponds to the Bragg diffraction regime. In the opposite limit a thin grating with $d = 12.5$ μm and $p = 5$ μm produces diffraction in the Raman–Nath regime at $\lambda = 0.488$ μm and $\kappa_{\text{thin}} \approx 0.012$.

To conclude, we have demonstrated that the layer undulations in the cholesteric cells can be used as switchable weakly polarization-dependent 2D diffraction gratings of both Raman–Nath and Bragg types. The periodic structure of the layer undulations and corresponding spatial modulation of an average refractive index in the plane of a cell allows us to produce diffraction patterns with a square-type arrangement of diffraction maxima. The spatial periodicity of the diffraction pattern can be changed and adjusted for different wavelengths by use of cholesterics of different pitch and by confining them into cells of different thicknesses. The intensities of the diffraction maxima can be continuously tuned by the applied voltage; the grating can be switched between the diffraction and no-diffraction states by use of pulses of ac voltage.

References

1. P. F. McManamon, T. A. Dorschner, D. L. Corkum, L. J. Friedman, D. S. Hobbs, M. Holz, S. Liberman, H. Q. Nguyen, D. P. Resler, R. C. Sharp, and E. A. Watson, Proc. IEEE **84,** 268 (1996).
2. A. Fernandez-Nieves, D. R. Link, D. Rudhardt, and D. A. Weitz, Phys. Rev. Lett. **92,** 105503 (2004).
3. D. Rudhardt, A. Fernandez-Nieves, D. R. Link, and D. A. Weitz, Appl. Phys. Lett. **82,** 2610 (2003).
4. E. Schulze and W. von Reden, Proc. SPIE **2408,** 113 (1995).
5. D. Subacius, P. J. Bos, and O. D. Lavrentovich, Appl. Phys. Lett. **71,** 1350 (1997).
6. D. Subacius, S. V. Shiyanovskii, Ph. Bos, and O. D. Lavrentovich, Appl. Phys. Lett. **71,** 3323 (1997).
7. S. W. Kang, S. Sprunt, and L. C. Chien, Appl. Phys. Lett. **76,** 3516 (2000).
8. A. Y.-G. Fuh, M.-S. Tsai, L.-J. Huang, and T.-C. Liu, Appl. Phys. Lett. **74,** 2572 (1999).
9. A. K. Ghosh, Y. Takanishi, K. Ishikawa, H. Takezoe, Y. Ono, and J. Kawamura, J. Appl. Phys. **95,** 5241 (2004).
10. I. I. Smalyukh, S. V. Shiyanovskii, and O. D. Lavrentovich, Chem. Phys. Lett. **336,** 88 (2001).
11. M. Kleman and O. D. Lavrentovich, *Soft Matter: An Introduction* (Springer, New York, 2003), p. 405.
12. T. Ishikawa and O. D. Lavrentovich, Phys. Rev. E **63,** 030501(R) (2001).
13. W. Helfrich, Appl. Phys. Lett. **17,** 531 (1970).
14. W. Helfrich, J. Chem. Phys. **55,** 839 (1971).
15. B. I. Senyuk, I. I. Smalyukh, and O. D. Lavrentovich, are preparing a paper titled "Undulations of lamellar liquid crystals in cells with finite surface anchoring."
16. I. I. Smalyukh and O. D. Lavrentovich, Phys. Rev. Lett. **90,** 085503 (2003).
17. O. D. Lavrentovich and D.-K. Yang, Phys. Rev. E **57,** R6269 (1998).
18. R. W. Boyd, *Nonlinear Optics* (Academic, San Diego, Calif., 1992), p. 318.